First-principle study on reactions of diamond (100) surfaces with hydrogen and methyl radicals

doi: 10.1103/PhysRevB.62.16995

First-principle study on reactions of diamond (100) surfaces with hydrogen and methyl radicals

Hiroyuki Tamura, Hui Zhou, Yoshihisa Hirano, Seiichi Takami, Momoji Kubo, Rodion V. Belosludov, and Akira Miyamoto
Department of Materials Chemistry, Graduate School of Engineering, Tohoku University, Aoba-yama 07, Sendai 980-8579, Japan

Akira Imamura
Hiroshima Kokusai Gakuin University, 6-20-1 Aki-ku Nakano, Hiroshima City 739-0321, Japan

Mikka N. Gamo and Toshihiro Ando
National Institute for Research in Inorganic Materials, 1-1 Namiki, Tsukuba, Ibaraki 305 0044, Japan
(Received 18 May 2000)

Density-functional calculations have been performed to investigate the reaction of diamond (100) surfaces with the hydrogen and methyl radical. In the present study, the plasma chemical-vapor deposition process using CH_4/H_2 gas was considered. The reactions with vapor CH_3 radicals on the terrace (dimer mechanism) and at the S_B step (trough mechanism) were investigated. The desorption of hydrogen from the step edge is easier than that from the terrace. It is expected that the concentration of the surface dangling bond at the step edge is higher than that on the terrace; therefore, the CH_3 radical is preferentially adsorbed at the step edge. The H abstraction from the CH_3 group at the step edge is easier than that on the terrace due to the steric repulsion with the adjacent H atom. The C_2H_5 group is formed on the surface as a by-product with the CH_3 adsorption at the CH_2 group.

I. INTRODUCTION

For the purpose of electronic applications of diamond thin films, it is important to establish high-quality crystal-growth techniques using chemical-vapor deposition (CVD). To realize a controllable process for high-quality diamond growth, the crystal-growth mechanisms in CVD must be elucidated. In the typical plasma CVD method, CH_4 and H_2 gases are supplied as sources for the diamond growth.[1] Hydrogen is believed to play an important role in this growth process.[2] Generally, the as-grown CVD diamond surfaces are terminated by hydrogen.[1] It is believed that the exchanges of the hydrogen atoms between the vapor and diamond surface proceed throughout the CVD growth. The crystal quality of diamond (100) surfaces tends to be higher than that of the (111) surfaces;[3] therefore, they are more important for the electronic applications.

The hydrogenated diamond (100) surfaces are generally terminated by 2×1 monohydride dimers.[1] The 2×1 and 1×2 domains of the dimer arrays coexist on the diamond (100) surfaces. The single layer steps perpendicular and parallel to the dimer bond of the upper terrace are called S_A and S_B, respectively.[4,5] It is known that the crystal quality can be improved by decreasing the CH_4/H_2 ratio in the source gas. For a low CH_4/H_2 ratio [e.g., 2% (Ref. 5)], the flat surfaces are grown along the dimer arrays, the so-called step-flow growth.[4,5] The step-flow growth selectively proceeds at the S_B step. For a high CH_4/H_2 ratio [e.g., 6% (Ref. 5)], the rate of nucleation on the terrace increases; therefore, the selectivity of the growth direction decreases.

Recently, the growth mechanisms of the diamond surfaces have been theoretically investigated using empirical potential,[6,7] semiempirical,[8,9] *ab initio* molecular-orbital[10,11] (MO), and density-functional (DFT) calculations,[12–14] and Monte Carlo (MC) simulations.[15,16] Harris and Goodwin investigated the chemical reactions of the hydrogenated diamond (100) surfaces with the CH_3 radical and hydrogen using molecular mechanics (MM) calculations.[6] As for the initial stage of the diamond (100) growth, two kinds of reaction mechanisms have been proposed.

The dimer mechanism has the following steps.

(1) The vapor H radical abstracts a H atom from the monohydride dimer.

(2) The vapor CH_3 radical is adsorbed on the surface dangling bond at the dimer.

(3) The H atom from the adsorbed CH_3 group is abstracted and the CH_2 group is formed.

(4) The CH_2 group is inserted into the dimer bond.

The trough mechanism is a reaction mechanism with the following steps.

(1) The CH_3 radical is adsorbed on the surface dangling bond at the step edge.

(2) The H atoms from the adsorbed CH_3 group and that from the adjacent monohydride dimer are abstracted.

(3) The CH_2 group at the step edge bridges with the adjacent dimer.

The effects of the CH_2 diffusion[8,9] and etching of the surface carbon[16] on the crystal growth have also been theoretically investigated. It has been expected that the step-flow growth proceeds via the trough mechanism while the dimer mechanism initiates the new nucleation on the flat terrace. It is important to understand how the crystal quality depends on the growth mechanisms. In particular, the factor that decreases the crystal quality must be elucidated in order to control the growth process. In the present study, the reaction mechanisms of the diamond (100) surfaces with hydrogen and methyl radicals have been studied using DFT calculations. The reactions during the initial stage of the growth

process on the terrace and that at the S_B step have been investigated.

II. METHODS

The DFT calculations were performed using the CASTEP code, in which a plane-wave basis set and a conjugated gradient electronic minimization[17] are used. In the present study, the electron-ion interactions are described using the norm-conserving nonlocal pseudopotentials[18] in real space.[19] The exchange and correlation energies were calculated using the Perdew-Wang form of the generalized gradient approximation (GGA).[20] The reliability of this method for the diamond surface reactions was proved in a previous study.[21] The details of the calculation are similar to those of the previous study. The plane-wave cutoff energy was set at 600 eV. Figure 1 shows the slab models of the hydrogenated diamond (100) surfaces represented by the 4×2 supercell. Figure 1(a) represents the 2×1 monohydride, where the dimer arrays periodically continue in the $\langle 11^{-}0\rangle$ direction. Figure 1(b) represents the S_B step at the $(2\times1)/(1\times2)$ domain boundary, where the 2×1 and 1×2 dimers are arranged side by side in the $\langle 110\rangle$ direction. The carbon atoms from the bottom layer and all of the cell parameters were fixed at the experimental value of the bulk crystal during the geometry optimizations. The dangling bonds of the bottom layer were terminated by the monohydride dimers. In this paper, the total spin of the even and odd electron system is 0 and 1, respectively, unless it is mentioned.

III. RESULTS AND DISCUSSION

A. Desorption of hydrogen

The adsorption and desorption of the hydrogen on the diamond surface have been exhaustively studied due to their importance in the CVD process.[3] In the present study, the hydrogen desorptions from the terrace and that from the S_B step edge have been investigated. The reaction energies (ΔH) of the H desorptions are summarized in Table I. The desorption of the H radical from the diamond surface is found to be endothermic. Under the CVD growth process, the H radicals in the vapor phase are considered to abstract the H atoms from the diamond surface. The ΔH of the H abstraction by the vapor H radical is more exothermic than the H radical desorption due to the ΔH of the H_2 formation of 103 kcal/mol (see Table II).

Figure 2(a) shows the model of the S_B step edge, in which H atoms are labeled as H1 to H5 for convenience. To compare the stability of the surface dangling bond, the H atoms were removed one by one and the total energy of the equilibrium geometries were calculated. The *p*-like orbital is found at the surface dangling bond in the single occupied level after one H atom is removed. Generally, the C-C lengths around the surface dangling bond decrease from those of the H-terminated surface and the C-C-C angles increase toward the plane structure. Although three-coordinated carbon atoms favor plane structures, they are strained by the surrounded lattice of the diamond. The three-coordinated carbon at the S_B step edge (H3 is removed) relaxes toward the plane structure. Therefore, the surface dangling bond at the step edge is found to be more stable than

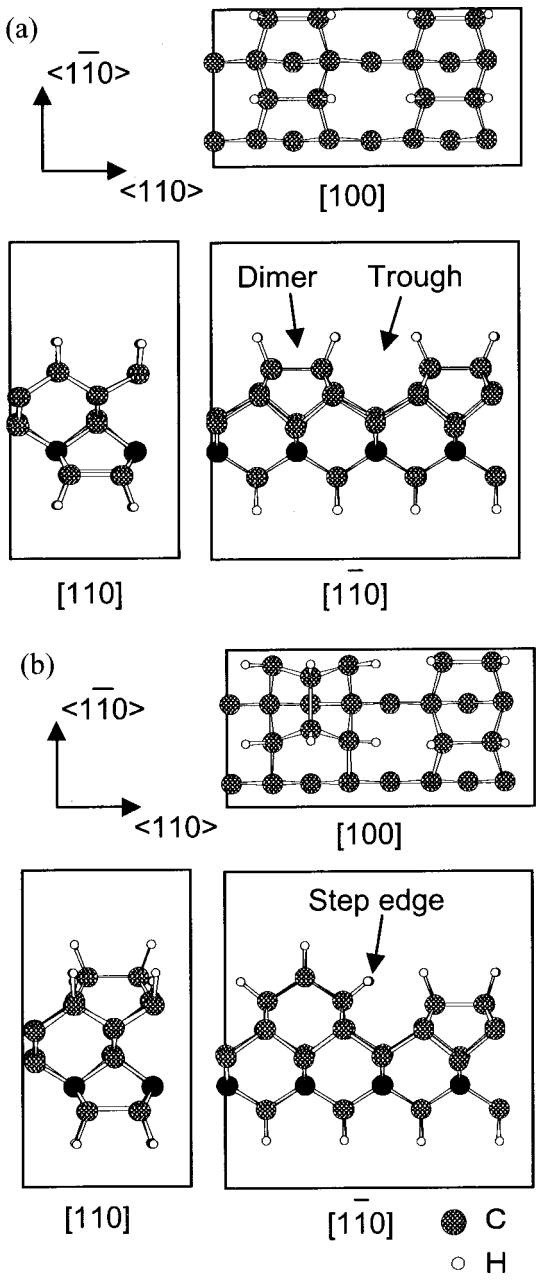

FIG. 1. Equilibrium geometries of the hydrogenated diamond (100) surfaces represented by the 4×2 supercell: (a) 2×1 dimer array on the flat terrace; (b) S_B step edge of a $(2\times1)/(1\times2)$ domain boundary, where the fixed carbon atoms are marked in black.

that at the dimer on the flat terrace. Since, the H atom at the step edge (H3) and that at the adjacent dimer (H5) is close to each other (1.80 Å), the steric repulsion is considered to be effective. The H desorption from the dimer adjacent to the S_B step (H5) is more favorable than that on the terrace due to the steric repulsion. In terms of equilibrium constants, the concentration of the surface dangling bond at the step edge is expected to be approximately $e^{10/RT}$ (150 at 1000 K) times larger than that on the terrace if the pre-exponential factor can be ignored. These results indicate that in the CVD process, the surface dangling bonds are preferentially formed at the S_B step edge.

The second abstractions of the H atom from the surface were also investigated. Figure 3 shows the schematic illus-

TABLE I. Reaction energies of hydrogen desorptions from the H-terminated diamond (100) surface.

Reaction	ΔH (kcal/mol)	
H radical desorption (diamond−H=diamond+H·)		
Dimer on the terrace [Fig. 4(b)]	104	
Dimer adjacent to the step [Fig. 5(b′)]	99	
Step edge [Fig. 5(b)]	94	
H abstraction by vapor H radical (diamond−H+H·=diamond+H_2)		
Dimer on the terrace [Fig. 4(b)]	1	
Dimer adjacent to the step [Fig. 5(b′)]	−4	
Step edge [Fig. 5(b)]	−9	
Second H abstraction (diamond−H+H·=diamond+H_2)		
Dimer on the terrace	−21	
H3→H4 [Fig. 2(b)]	1 (singlet)	−9 (triplet)
H3→H1 [Fig. 2(c)]	−28	
Third H abstraction (diamond−H+H·=diamond+H_2)		
H3,H1→H2 [Fig. 2(d)]	−3	
H3,H1→H4 [Fig. 2(e)]	−9	
Fourth H abstraction (diamond−H+H·=diamond+H_2)		
H3,H1,H4→H2 [Fig. 2(f)]	−34	
H_2 desorption (diamond−2H=diamond+H_2)		
Dimer on the terrace	84	
Step edge [Fig. 2(b)]	95 (singlet)	85 (triplet)
Side bond [Fig. 2(c)]	66	
Second H_2 desorption (diamond−2H=diamond+H_2)		
H1-H3 [Fig. 2(c)]→H2-H4 [Fig. 2(f)]	61	

trations of the orbitals near the highest occupied level. In these orbitals, the charge density generally distributes around the surface dangling bonds and is delocalized if they are close to each other. After the second H abstraction from the monohydride dimer, the clean dimer is formed and the C-C length is decreased to 1.36 Å. The ΔH of the second H abstraction from the monohydride dimer (−21 kcal/mol) is lower than that of the first one (1 kcal/mol). This difference is considered to originate from the stabilization due to the π bond formation at the clean dimer. A similar tendency was also found in the *ab initio* calculations using cluster models.[22] It is believed that this tendency enhances the associative desorption of hydrogen from the dimer and it contributes to the first-order kinetics of the H_2 thermal desorption.[3]

The adjacent dangling bonds are created by the second H abstraction from the step edge (abstract H4 after H3). Figure 2(b) shows the equilibrium geometry of the adjacent edge dangling bonds. The carbons at the step edge and also the carbon atoms from the lower two layers deviate from the sp^3 structure toward the plane structure. Therefore, the C-C lengths between the first and second lower layer increase from the original C-C length of the diamond [see Fig. 2(b)]. The equilibrium geometry of the edge dangling bond with total spin=2 (triplet) is found to be more stable than that with spin=0 (singlet). In the case of the singlet state, the ΔH of the second H abstraction (H4) of 1 kcal/mol is higher than that of the first one (H3) of −9 kcal/mol. In this case, the antibonding orbital (i.e., there is a node in the wave function between the two dangling bonds) is found in the highest occupied level [Fig. 3(a′)], and the bonding orbital is found in the lowest unoccupied level [Fig. 3(a)]. This is in contrast to the clean dimer bond in which the bonding π and the antibonding π^* orbitals are found in the highest occupied and the lowest unoccupied level, respectively.[23] In the case of the triplet state, the ΔH of the second H abstraction from the step edge (−9 kcal/mol) is as large as that of the first one. Therefore, the triplet state is more stable than the singlet

TABLE II. Reaction energies of the dimer mechanism on the flat terrace.

Reaction	ΔH (kcal/mol)
Creation of surface dangling bond	
Fig. 4(a)+H·=Fig. 4(b)+H_2	1
CH_3 adsorption	
Fig. 4(b)+CH_3·=Fig. 4(c)	−84
CH_4 desorption	
Fig. 4(c)+H·=Fig. 4(b)+CH_4	−23
H abstraction from CH_3 group	
Fig. 4(c)+H·=Fig.4(d)+H_2	−5
Dimer bond dissociation	
Fig. 4(d)=Fig. 4(e)	7
CH_2 insertion into dimer bond	
Fig. 4(e)=Fig. 4(f)	−18
Dihydride formation	
Fig. 4(e)+H·=Fig. 4(h)	−82
H adsorption after CH_2 insertion	
Fig. 4(f)+H·=Fig. 4(g)	−95
C_2H_5 formation	
Fig. 4(d)+CH_3·=Fig. 4(i)	−77
C_2H_6 desorption	
Fig. 4(i)+H·=Fig. 4(b)+C_2H_6	−30

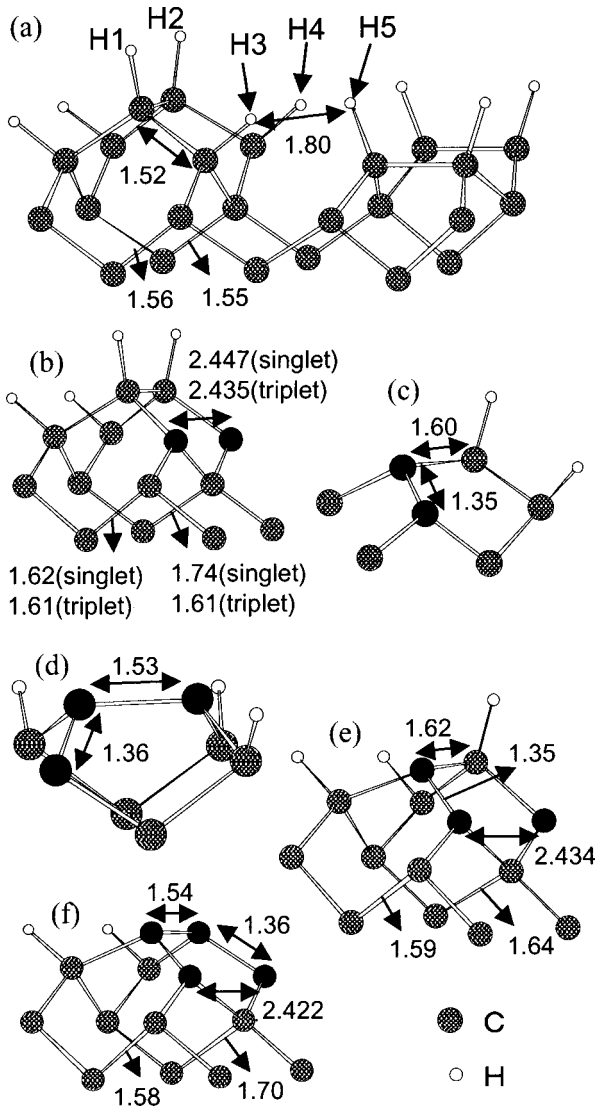

FIG. 2. (a) Equilibrium geometry (in Å) of the S_B step edge, where H1-H2, H3-H4, and H5 indicate the H atoms from the upper dimer, from the S_B step edge, and from the adjacent dimer, respectively. Equilibrium geometries (in Å) after (b) H3-H4, (c) H1-H3, (d) H1-H2-H3, (e) H1-H3-H4, and (f) H1-H2-H3-H4 are desorbed, where the dangling bonds are marked in black.

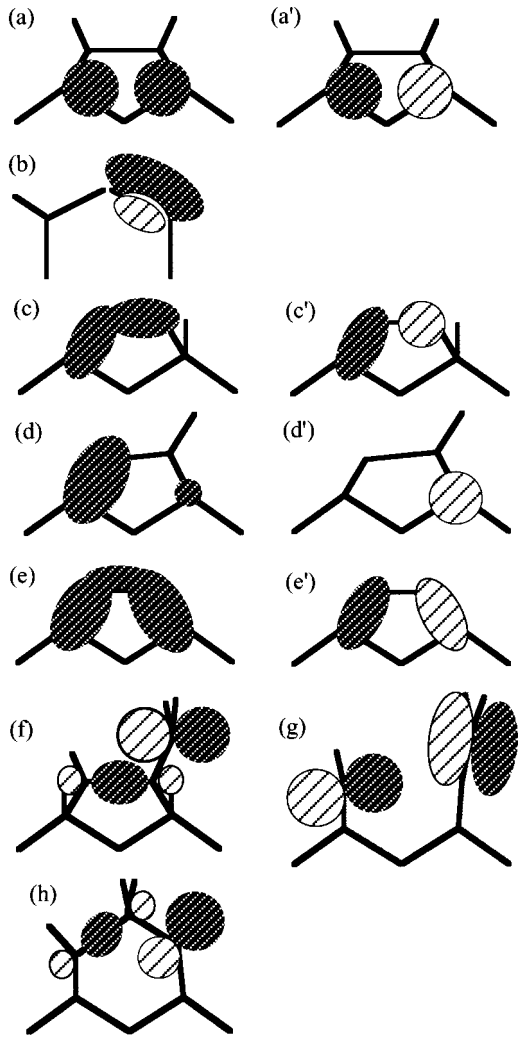

FIG. 3. Schematic illustrations of the orbitals near the highest occupied level; (a) bonding and (a′) antibonding orbitals between the dangling bonds at the step edge; (b) the π bonding orbital at the side bond (highest occupied orbital); (c) the second highest occupied and (c′) single occupied orbital after H1-H2-H3 are desorbed; (d) the second highest occupied and (d′) single occupied orbital after H1-H3-H4 are desorbed; (e) the second highest and (e′) highest occupied orbital after H1-H2-H3-H4 are desorbed; the single occupied orbital of (f) the CH_2 group at the dimer, (g) the ethylene-like structure, and (h) the CH_2-inserted dimer. For simplification, the phase of the wave function is represented by the two kinds of patterns with the node between the different patterns.

state for the adjacent dangling bonds at the step edge. In the case of the triplet state, both the bonding [Fig. 3(a)] and the antibonding [Fig. 3(a′)] orbitals are occupied by one electron. The distance between the dangling bonds at the step edge (2.4 Å) is larger than that of the clean dimer (1.36 Å). Therefore, the stabilization due to π bond formation is ineffective for the adjacent dangling bond at the step edge. This is in contrast to the clean dimer bond, which is stabilized by the π bond.

Figure 2(c) shows the equilibrium geometry after the H desorption from the step edge (H3) and the upper dimer (H1). In the case of the H abstraction from the upper dimer, which is adjacent to the edge dangling bond (i.e., abstract H1 after H3), the ΔH of the second H abstraction from the dimer of -28 kcal/mol is lower than that of the first one on the terrace of 1 kcal/mol. In this case, the π bond orbital is found between two dangling bonds [Fig. 3(b)]; therefore, the length of the C-C bond, namely the side bond, is decreased to 1.35 Å [Fig. 2(c)]. Therefore, the π bond formation at the side bond is expected to enhance the associative desorption of hydrogen similar to the dimer bond.

In the experimental measurements of the thermal desorptions of hydrogen from diamond (100), only the H_2 molecules are observed due to the associative desorption of the H atoms.[3] The ΔH of the molecular desorption of H_2 is less endothermic than that of the H radical desorption (see Table I). The desorption of the H_2 molecule from the side bond (H1-H3) is found to be the most favorable. In this case, both the π bond formation and the relaxation toward the plane structure contribute to the stabilization. Su and Lin investigated the thermal desorption of H_2 from diamond (100) using temperature programmed desorption (TPD) and three types

of peaks for the H_2 desorption were observed.[24] They also reported that the peak at the highest temperature, for which the activation energy (E_{act}) is 80 kcal/mol and the rate is first order, corresponds to the H_2 desorption from the 2×1 dimer. The experimental E_{act} is close to the calculated ΔH of the H_2 desorption from the 2×1 dimer of 84 kcal/mol. The reason for the first-order kinetics is explained that the H atoms are associatively desorbed from the same dimer rather than abstracted by the H atom from another dimer. The TPD peaks at the lower temperature were supposed to be caused by the H_2 desorption from the dihydride and that from the step edge.[24] Our calculations indicate that the H_2 desorption from the side bond [Fig. 2(c)] is easier than the other sites and so it is supposed to correspond to the TPD peak at the lowest temperature.

We also investigated the third and fourth H abstractions. The ΔH of the H abstractions in Table I were calculated using the lowest-energy path, i.e., the ΔH of the third H abstraction was calculated from Fig. 2(c). Figure 2(d) is the equilibrium geometries after H3, H1, and H2 are desorbed. In the single occupied orbital of this geometry, the π bond is found at the side bond, while the node is found at the dimer bond [Fig. 3(c′)]. The second highest occupied orbital is found to be bonding for both the dimer and the side bond [Fig. 3(c)]. The dimer bond length of 1.53 Å is longer than that of the clean dimer on the terrace of 1.36 Å, because one electron occupies the antibonding orbital. These results indicate that the π bond is preferentially formed at the side bond versus the dimer bond due to the shorter C-C length.

Figure 2(e) shows the equilibrium geometry after H3, H1, and H4 are desorbed. The single occupied orbital of this geometry is found to be localized at the edge dangling bond [Fig. 3(d′)], which is almost similar to that of the isolated edge dangling bond. In the second highest occupied orbital, the π bond is found at the side bond [Fig. 3(d)]. In this case, the delocalization of the orbital does not significantly contribute to the energetics. Therefore, the ΔH of the third H abstraction is as large as that of the first one at the step edge.

Figure 2(f) shows the equilibrium geometry after H3, H1, H4, and H2 are desorbed. The ΔH of the fourth H abstraction is found to be the most exothermic (-34 kcal/mol). In the highest occupied orbital, the π bond is found at each of the side bonds and the node is found at the dimer bond [Fig. 3(e′)]. In the second highest occupied orbital, the π bonds are found not only at the side bond but also at the dimer bond [Fig. 3(e)]. In this case, the π bond is also preferentially formed at the side bond rather than at the dimer bond. The C-C distance of the dimer is longer than that of the clean dimer on the terrace due to the contribution of the antibonding orbital. As for the molecular desorptions of H_2, the ΔH of the second H_2 desorption from the side bond (61 kcal/mol) is lower than that of the first one (66 kcal/mol). In this case, the π bond formation at the dimer does not enhance the second H_2 desorption very much, because the antibonding orbital is also occupied.

The ΔH of abstraction of the surface hydrogen by the vapor H radical is much more exothermic than either the thermal desorptions of the H radicals or that of the H_2 molecules. Therefore, in the CVD process, the surface dangling bonds are considered to be created by the vapor H radicals. The ΔH of the H radical adsorption is more exothermic than that of the H abstraction for any sites. In the typical plasma CVD process, the large amount of the vapor H radical is expected to be readily adsorbed at the surface dangling bonds. Therefore, most of the surface area is regarded to be H-terminated though the exchange of hydrogen between the vapor and the surface proceeds during the CVD growth process. The concentration of the surface dangling bonds at the step edge is considered to be higher than that on the terrace. It is expected that a large amount of vapor H radical decreases the concentration of the surface dangling bonds and increases the selectivity of the chemical reactions. In the recent theoretical investigation of the Si (100),[25] the H adsorption at the step edge is more favorable than that on the terrace in contrast to the diamond (100).

B. Dimer mechanism

Recently, based on theoretical investigations,[6–16] it has been suggested that the nucleation on the terrace of diamond (100) occurs with CH_2 insertion into the dimer bond via several reaction steps, e.g., the so-called dimer mechanism. However, the reaction mechanisms are considered more controversial.

In the present calculations, the ΔH of the reactions have been calculated while the E_{act} of the reactions have not been investigated. The calculated reaction path and the reaction energies are summarized in Fig. 4 and Table II, respectively. The CH_3 radical is expected to be readily adsorbed at the dangling bond on the terrace [Fig. 4(c)]. The ΔH of the CH_3 adsorption is found to be -84 kcal/mol, which is more exothermic than the result of the non-self-consistent local-density approximation (LDA) calculation by Alfonso, Yang, and Drabold.[13]

The H atom from the adsorbed CH_3 group is abstracted by the vapor H radical and a CH_2 group is formed [Fig. 4(d)]. The ΔH of the H abstraction from the adsorbed CH_3 group (-5 kcal/mol) is more exothermic than that from the dimer on the terrace (1 kcal/mol). The CH_3 group is considered to be desorbed as a CH_4 molecule with the vapor H radical. The ΔH of CH_4 desorption is found to be exothermic and it may competitively occur with the H abstraction.

After H abstraction from the CH_3 group, the dimer bond length slightly increases and the C-CH_2 bond length slightly decreases [Fig. 4(d)]. In this geometry, the single occupied orbital distributes at the CH_2 and dimer bond [Fig. 3(f)]. Another local minimum geometry is found after the dissociation of the dimer bond in which an ethylenelike structure is found [Fig. 4(e)]. The ΔH of the dimer bond dissociation is endothermic with a value of 7 kcal/mol. The single occupied orbital of this geometry distributes at the CH_2 of the ethylenelike structure and the adjacent three-coordinated carbon in which the node is found between them [Fig. 3(g)]. The C-C length of the ethylenelike structure decreases to 1.33 Å after the dimer dissociation, because the charge density that contributes the dimer bond transfers to the π bond of the ethylenelike structure.

The ΔH of the CH_2 insertion into the dimer bond [Fig. 4(f)] is found to be exothermic. After the CH_2 insertion, a new surface dangling bond is formed at the side of the dihydride. The single occupied orbital distributes at the dangling bond and the CH_2-CH bond [Fig. 3(h)]. In terms of the

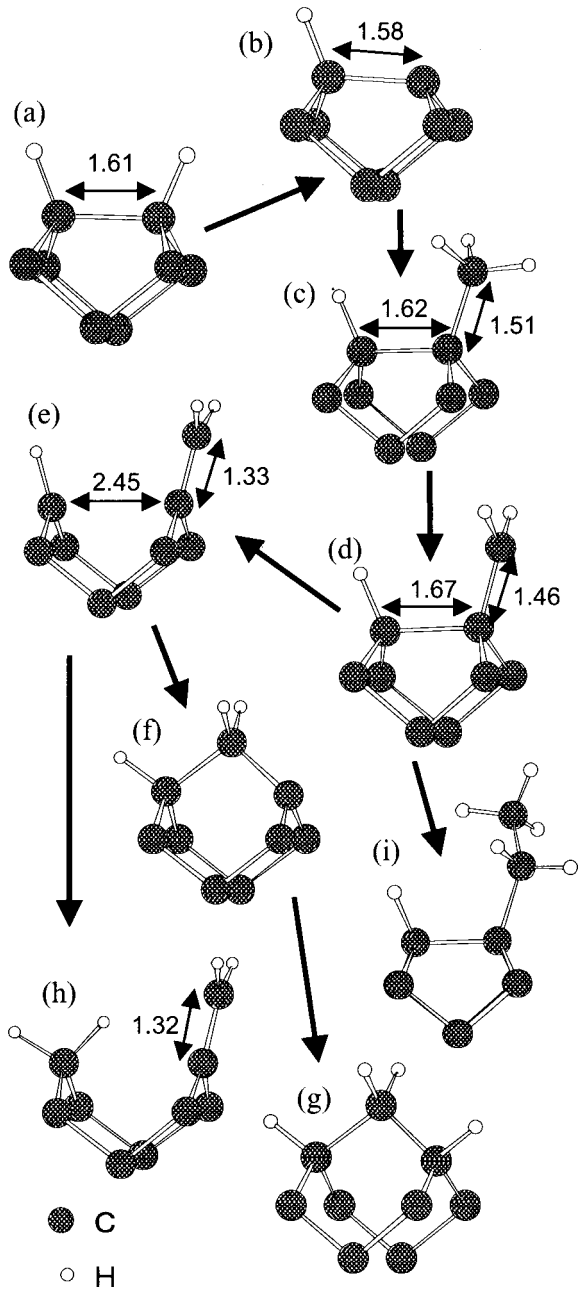

FIG. 4. Reaction path of the dimer mechanism on the terrace. Equilibrium geometries (in Å) of the (a) 2×1 dimer, (b) the dangling bond at the dimer, (c) the CH_3 group at the dimer, (d) the CH_2 group at the dimer, (e) the ethylenelike structure, (f) the CH_2-inserted dimer, (g) the CH_2-inserted dimer after the H terminate, (h) the dihydride adjacent to the ethylenelike structure, and (i) the C_2H_5 group at the dimer, where only the geometries around the dimer are shown.

frontier-orbital theory,[26] the change in the single occupied orbital with the CH_2 insertion indicates the symmetry forbidden; therefore, a considerable E_{act} is predicted to be necessary. In the non-self-consistent LDA calculations by Kaukonen *et al.*,[14] the E_{act} of the CH_2 insertion is found to be 40 kcal/mol. They also reported that boron doping decreases the E_{act} of the CH_2 insertion due to the charge transfer from the surface to the boron acceptor level.

The ΔH of H adsorption at the surface dangling bond after the CH_2 insertion [Fig. 4(g)] was found to be -95 kcal/mol. The ΔH of the abstraction of this H atom (-8 kcal/mol) is close to that from the step edge (-9 kcal/mol) and so the trough mechanism, which is described later, is expected to proceed from here. The CH_2 insertion must occur in the lifetime of the dangling bond at the CH_2 group because it readily reverses to the CH_3 group with the adsorption of a vapor H radical (in this case, the ΔH is -98 kcal/mol). Moreover, the reverse reaction of the CH_2 insertion is also considered to occur during the CVD process.[16]

The dihydride structure is formed via the H radical adsorption at the three-coordinated carbon adjacent to the ethylenelike structure [Fig. 4(h)]. The ΔH of this reaction is found to be exothermic with a value of -82 kcal/mol. Therefore, this intermediate geometry can be also formed with a considerable probability. This dihydride prevents both the CH_2 insertion and the reformation of the dimer bond. This geometry is less stable than the CH_2-inserted dimer [Fig. 4(g)], where the stoichiometry is equal. These two geometries [Figs. 4(g) and 4(h)] are considered to be reversible in the CVD process, although energy barriers exist in the reaction path between them.

If the CH_2 group adsorbs the vapor CH_3 radical, the C_2H_5 group is formed at the dimer [Fig. 4(i)]. The ΔH of the C_2H_5 group formation is more exothermic than that of the CH_2 insertion into the dimer bond. Moreover, the CH_2 insertion is considered to be the rate-determining step of the dimer mechanism due to its high E_{act}.[14] Therefore, the C_2H_5 group can be formed before the CH_2 insertion with a considerable probability. As the vapor CH_3 concentration increases, the formation of the C_2H_5 group is expected to increase. Once the C_2H_5 group is formed, the CH_2 insertion into the dimer bond is inhibited. Therefore, the C_2H_5 group is considered to be one of the by products, which disturbs the crystal growth. This idea is in agreement with the experimental fact that the crystal quality decreases as the CH_4/H_2 ratio in the source gas increases. The C_2H_5 group is considered to be desorbed by the vapor H radical, where the ΔH of the C_2H_6 desorption is found to be -30 kcal/mol. Therefore, a large amount of H radical is expected to remove such a by-product during the CVD process.

C. Trough mechanism

The trough mechanism[6] was investigated using the 4×2 supercell which includes the S_B step of the $(2\times1)/(1\times2)$ domain boundary [Fig. 1(b)]. The reaction path and the reaction energies are summarized in Figs. 5 and Table III, respectively. The chance of CH_3 adsorption at the step edge is expected to be higher than that at the dimer due to the higher concentration of the surface dangling bonds. The ΔH of the CH_3 adsorption at the step edge of -46 kcal/mol and that at the adjacent dimer site of -68 kcal/mol are less exothermic than that at the dimer on the terrace of -84 kcal/mol. For the CH_3 group at the step edge and at the adjacent dimer, the H atom from the CH_3 group is close to the adjacent H atom [see Figs. 5(c) and 5(c′)]. In particular, the torsion angle of the CH_3 group at the step edge deviates from that of the trans-conformation (60°) by approximately 25° to decrease the steric repulsion. In the case of the CH_3 group on the terrace [Fig. 4(c)], the distance to the adjacent H atom is larger (1.68 Å) and it keeps the trans-conformation. These

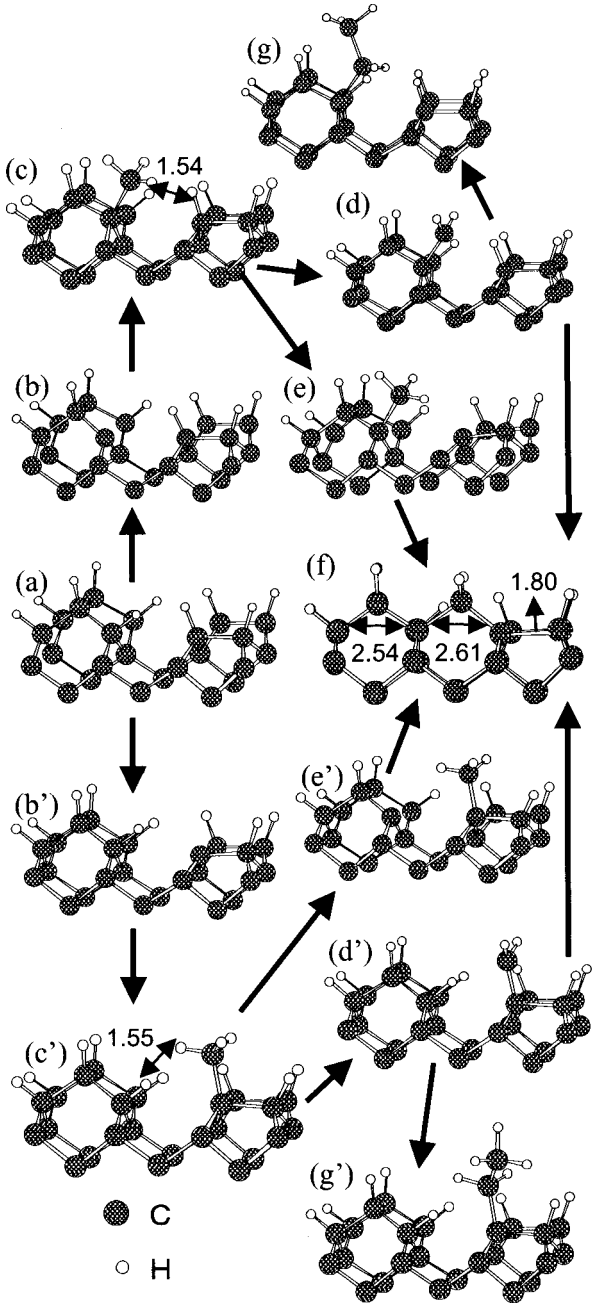

FIG. 5. Reaction path of the trough mechanism at the S_B step edge. Equilibrium geometries (in Å) of the (a) H-terminated S_B step, the dangling bond (b) at the step edge and (b′) at the adjacent dimer, the CH_3 group (c) at the step edge and (c′) at the adjacent dimer, the CH_2 group (d) at the step edge and (d′) at the adjacent dimer, the dangling bond (e) at the dimer and (e′) at the step edge adjacent to the CH_3 group, (f) the CH_2 bridging across the trough, and the C_2H_5 group (g) at the step edge and (g′) at the adjacent dimer, where only the geometries of the upper layers are shown.

TABLE III. Reaction energies of the trough mechanism at the S_B step.

Reaction	ΔH (kcal/mol)
Creation of surface dangling bond	
Fig. 5(a)+H·=Fig. 5(b)+H_2	−9
Fig. 5(a)+H·=Fig. 5(b′)+H_2	−4
CH_3 adsorption	
Fig. 5(b)+CH_3·=Fig. 5(c)	−46
Fig. 5(b′)+CH_3·=Fig. 5(c′)	−68
CH_4 desorption	
Fig. 5(c)+H·=Fig. 5(b)+CH_4	−61
Fig. 5(c′)+H·=Fig. 5(b′)+CH_4	−39
H abstraction from CH_3 group	
Fig. 5(c)+H·=Fig. 5(d)+H_2	−18
Fig. 5(c′)+H·=Fig. 5(d′)+H_2	−9
Abstraction of adjacent H	
Fig. 5(c)+H·=Fig. 5(e)+H_2	−16
Fig. 5(c′)+H·=Fig. 5(e′)+H_2	−14
CH_2 bridging	
Two-step Fig. 5(c)+2H·=Fig. 5(f)+2H_2	−101
Two-step Fig. 5(c′)+2H·=Fig. 5(f)+2H_2	−80
One-step Fig. 5(c)=Fig. 5(f)+H_2	2
One-step Fig. 5(c′)=Fig. 5(f)+H_2	23
C_2H_5 formation	
Fig. 5(d)+CH_3·=Fig. 5(g)	−60
Fig. 5(d′)+CH_3·=Fig. 5(g′)	−69
C_2H_6 desorption	
Fig. 5(g)+H·=Fig. 5(b)+C_2H_6	−72
Fig. 5(g′)+H·=Fig. 5(b′)+C_2H_6	−44

results indicate that the CH_3 group at the step edge is more unstable than that on the terrace due to the steric repulsion. Therefore, the ΔH that desorbs the CH_4 molecule from the step edge is more exothermic than that from the terrace.

The ΔH of the H abstraction from the adsorbed CH_3 group at the step edge [Fig. 5(d)] of −18 kcal/mol and that at the adjacent dimer [Fig. 5(d′)] of −9 kcal/mol are more exothermic than that on the terrace [Fig. 4(d)] of −5 kcal/mol due to the steric repulsion. The ΔH of the H abstraction from the dimer adjacent to the CH_3 group [Fig. 5(e)] and that from the step edge adjacent to the CH_3 group [Fig. 5(e′)] are more exothermic than those without the adjacent CH_3 group. These results indicate that at the S_B step edge, the steric repulsion between H atoms accelerates the H desorptions.

The CH_2 group bridges across the trough with the second H abstraction [Fig. 5(f)]. In this geometry, the C-C length of the adjacent dimer is elongated to 1.8 Å due to the increase in the tensile stress. The bridging can occur in the lifetime of the dangling bond; in other words, the second H must be abstracted before another dangling bond adsorbs H again. The ΔH of the molecular desorptions of H_2 with the CH_2 bridging are much less endothermic than either that from the dimer or that from the step edge; therefore, the thermal desorption of H_2 is considered to be relatively easy. The ΔH of the bridging with the two-step H abstraction is more exothermic than that with the one-step H_2 thermal desorption. Therefore, in the CVD process with a large amount of H radicals, the CH_2 bridging is considered to occur via the two-step H abstraction.

If the CH_3 radical is adsorbed at the CH_2 group before the bridging, the C_2H_5 group is formed [Figs. 4(g) and 4(g′)]. This C_2H_5 group inhibits the bridging of CH_2 across the trough. The ΔH of C_2H_5 formation at the step edge and that at the adjacent dimer are less exothermic than that on the terrace due to the steric repulsion. In particular, the torsion angle of the C_2H_5 group at the step edge [Fig. 4(g)] deviates

by approximately 60° (i.e., cis-conformation). The ΔH of C_2H_6 desorption from the step edge is more exothermic than that from the terrace due to its unstability. These results indicate that the C_2H_5 formation at the S_B step is relatively unfavorable; therefore, the selectivity of the growth reactions at the S_B step is expected to be higher than that on the terrace.

IV. CONCLUSIONS

The reactions of the diamond (100) surface with hydrogen and methyl radicals have been investigated using the DFT calculations with the GGA level and norm-conserving pseudopotentials. The present study revealed the growth mechanisms of the CVD diamond (100) on the terrace and at the step edge as follows.

(1) The surface dangling bond at the S_B step edge is more stable than that on the terrace due to the relaxation toward the plane structure.

(2) The second H abstraction becomes easier if the dangling bonds are closer to each other to form the π bond. The thermal desorption of H_2 from the side bond [H1-H3 in Fig. 2(a)] is the most favorable because of the close C-C distance.

(3) The CH_2 insertion into the dimer bond proceeds via the CH_3 adsorption, H abstraction, and dimer dissociation with the formation of the ethylenelike structure. If the CH_3 radical is adsorbed on the CH_2 group, the C_2H_5 group is formed and the CH_2 insertion is inhibited.

(4) The adsorbed CH_3 at the S_B step edge is closer to the adjacent H atom than that on the terrace; therefore, the H desorption is easier due to the steric repulsion.

(5) The C_2H_5 group formation at the step edge inhibits the CH_2 bridging across the trough. This C_2H_5 group is more unstable than that on the terrace due to the steric repulsion.

In the experimental observations, the step-flow growth selectively proceeds at the S_B step for a low CH_4/H_2 ratio, while the nucleation on the terrace increases for a high CH_4/H_2 ratio.[5] This tendency is considered to originate from the difference in the reaction mechanisms on the terrace and those at the step edge. In the CVD process with a large amount of H radicals, the concentration of surface dangling bonds is expected to be very low and it mainly distributes at the S_B step edge. At the S_B step edge, the CH_3 is expected to be preferentially adsorbed due to the higher concentration of the surface dangling bonds. The rate of some reactions in the step-flow growth is considered to be independent on the concentration of the vapor CH_3 radicals. For example, the rate of the CH_2 bridging [Figs. 5(c) to 5(f)] only depends on the reaction with H. Moreover, the total length of the S_B step on the surface is relatively small[4,5] and the new S_B step does not appear until the entire reaction cycle is completed. Therefore, even if the concentration of the vapor CH_3 radicals increases, the rate of the step-flow growth does not increase very much. The oversupplied CH_3 radical is expected to increases the nucleation on the terrace. The increase in the CH_3 radical concentration is considered to rather enhance the C_2H_5 group formation than the CH_2 insertion on the terrace. In the case of the low CH_3 concentrations, the CH_2 insertion is considered to proceed before the formation of the C_2H_5 group. As long as the crystal growth proceeds at the S_B step, the formation of the C_2H_5 group is expected to be more unfavorable due to the steric repulsions. Therefore, in order to produce the high-quality CVD diamond, it is important to decrease the CH_4/H_2 ratio to increase the selectivity of the growth reactions.

It is known that the growth mechanisms of diamond depend not only on the CH_4/H_2 ratio but also on some impurities.[14,27] Therefore, the investigation of the effect of impurities on the growth mechanisms is now in progress.

[1] F. G. Celii and J. E. Butler, Annu. Rev. Phys. Chem. **42**, 643 (1991).

[2] B. B. Pate, Surf. Sci. **165**, 83 (1986).

[3] M. P. D'Evelyn, *Handbook of Industrial Diamonds and Diamond Films*, edited by M. A. Prelas, G. Popovici, and L. K. Bigelow (Dekker, New York, 1998), pp. 89–146.

[4] H. Kawarada, H. Sasaki, and A. Sato, Phys. Rev. B **52**, 11 351 (1995).

[5] T. Tsuno, T. Tomikawa, S. Shikata, T. Imai, and N. Fujimori, Appl. Phys. Lett. **64**, 572 (1994).

[6] S. J. Harris and D. G. Goodwin, J. Phys. Chem. **97**, 23 (1993).

[7] D. R. Alfonso, S. E. Ulloa, and D. W. Brenner, Phys. Rev. B **49**, 4948 (1994).

[8] S. Skokov, B. Weiner, and M. Frenklach, J. Phys. Chem. **98**, 7073 (1994); **99**, 5616 (1994).

[9] M. Frenklach, S. Skokov, and B. Weiner, Nature (London) **372**, 535 (1994).

[10] T. I. Hukka, T. A. Pakkanen, and M. P. D'Evelyn, Surf. Sci. **359**, 213 (1996).

[11] K. Larsson, S. Lunell, and J. O. Carlsson, Phys. Rev. B **48**, 2666 (1993).

[12] M. H. Tsai and Y. Y. Yeh, Phys. Rev. B **58**, 2157 (1998).

[13] D. R. Alfonso, S. H. Yang, and D. A. Drabold, Phys. Rev. B **50**, 15 369 (1994).

[14] M. Kaukonen, P. K. Sitch, G. Jungnickel, R. M. Nieminen, S. Poykko, D. Porezag, and Th. Frauenheim, Phys. Rev. B **57**, 9965 (1998).

[15] E. J. Dawnkaski, D. Srivastava, and B. J. Garrison, J. Chem. Phys. **102**, 9401 (1995); **104**, 5997 (1996).

[16] C. C. Battaile, D. J. Srolovitz, I. I. Oleinik, D. G. Pettifor, A. P. Sutton, S. J. Harris, and J. E. Butler, J. Chem. Phys. **111**, 4291 (1999).

[17] M. P. Teter, M. C. Payne, and D. C. Allan, Phys. Rev. B **40**, 12 255 (1989).

[18] D. R. Hamann, M. Schlüter, and C. Chiang, Phys. Rev. Lett. **43**, 1494 (1979). G. B. Bachelet, D. R. Hamann, and M. Schlüter, Phys. Rev. B **26**, 4199 (1982).

[19] R. D. King-Smith, M. C. Payne, and J. S. Lin, Phys. Rev. B **44**, 13 063 (1991).

[20] K. Burke, J. P. Perdew, and M. Levy, *Modern Density Functional Theory: A Tool for Chemistry*, edited by J. M. Seminario and P. Politzer, Theoretical and Computational Chemistry Vol. 2 (Elsevier, New York, 1995), pp. 29–74.

[21] H. Tamura, H. Zhou, K. Sugisako, Y. Yokoi, S. Takami, M.

Kubo, K. Teraishi, A. Miyamoto, A. Imamura, M. N. Gamo, and T. Ando, Phys. Rev. B **61**, 11 025 (2000).
[22] T. I. Hukka, T. A. Pakkanen, and M. P. D'Evelyn, J. Phys. Chem. **98**, 12 420 (1994).
[23] J. Furthmuller, J. Hafner, and G. Kresse, Phys. Rev. B **53**, 7334 (1996).
[24] C. Su and J. C. Lin, Surf. Sci. **406**, 149 (1998).
[25] P. Kratzer, E. Pehlke, M. Scheffler, M. B. Raschke, and U. Höfer, Phys. Rev. Lett. **81**, 5596 (1998); E. Pehlke and P. Kratzer, Phys. Rev. B **59**, 2790 (1999).
[26] I. Fleming, *Frontier Orbitals and Organic Chemical Reactions* (William Clowes & Sons, London, 1976).
[27] I. Sakaguchi, M. N.-Gamo, Y. Kikuchi, E. Yasu, H. Haneda, T. Suzuki, and T. Ando, Phys. Rev. B **60**, 2139 (1999).